Effects of exposure parameters and slice thickness on detecting clear and unclear mandibular canals using cone beam CT

ガイナー, ハサ

https://doi.org/10.15017/1928640

出版情報：九州大学, 2017, 博士（歯学）, 論文博士
バージョン：

Dentomaxillofacial Radiology (2017) 46, 20160315

birpublications.org/dmfr

RESEARCH ARTICLE

Effects of exposure parameters and slice thickness on detecting clear and unclear mandibular canals using cone beam CT

[1]Gainer R Jasa, [2]Mayumi Shimizu, [3]Kazutoshi Okamura, [4]Kenji Tokumori, [2]Yohei Takeshita, [3]Warangkana Weerawanich and [3]Kazunori Yoshiura

[1]Oral Radiology Division, University of the Republic, Montevideo, Uruguay; [2]Department of Oral and Maxillofacial Radiology, Kyushu University Hospital, Fukuoka, Japan; [3]Department of Oral and Maxillofacial Radiology, Faculty of Dental Science, Kyushu University, Fukuoka, Japan; [4]Department of Radiological Technology, Faculty of Fukuoka Medical Technology, Teikyo University, Fukuoka, Japan

Objectives: The purpose of this study was to clarify the effects of exposure parameters and image-processing methods when using CBCT to detect clear and unclear mandibular canals (MCs).
Methods: 24 dry half mandibles were divided into 2 groups with clear and unclear MCs based on a previous CBCT study. Mandibles were scanned using a CBCT system with varying exposure parameters (tube voltages 60 kV, 70 kV and 90 kV; and tube currents 2 mA, 5 mA, 10 mA and 15 mA) to obtain a total of 144 scans. The images were processed with different slice thicknesses using ImageJ software (National Institutes of Health, Bethesda, MD). Five radiologists evaluated the cross-sectional images of the first molar region to detect the MCs. The diagnostic accuracy of varying exposure parameters and image-processing conditions was compared with the area under the curve (Az) in receiver-operating characteristic analysis.
Results: The Az values for clear MCs were higher than those for unclear MCs ($p < 0.0001$). With increasing exposure voltages and currents, Az values increased, but no significant differences were found with high voltages and currents in clear MCs ($p = 1.0000$ and $p = 0.9340$). The Az values of serial images were higher than those of overlaid images ($p < 0.0001$), and those for thicker slices were higher than those for thinner slices ($p < 0.0001$).
Conclusions: Our findings indicate that detection of unclear MCs requires either higher exposure parameters or processing of the images with thicker slices. To detect clear MCs, lower exposure parameters can be used.
Dentomaxillofacial Radiology (2017) **46**, 20160315. doi: 10.1259/dmfr.20160315

Cite this article as: Jasa GR, Shimizu M, Okamura K, Tokumori K, Takeshita Y, Weerawanich W, et al. Effects of exposure parameters and slice thickness on detecting clear and unclear mandibular canals using cone beam CT. *Dentomaxillofac Radiol* 2017; **46**: 20160315.

Keywords: CBCT; mandible; computer-assisted image processing; image quality

Introduction

Implant surgery is a common procedure in clinical dental practice, and different imaging methods are used in planning.[1–4] When the mandibular molar region is the implant receptor site, it is important to accurately establish the location of the mandibular canals (MCs) to avoid vascular trauma or nerve damage.[5]

Panoramic radiography is usually the first radiographic method used to evaluate the location of the MC.[6–9] However, the information it provides is only two-dimensional and the images are distorted, often resulting in miscalculation of the location of the MC.[4,7]

CBCT and CT are the most common diagnostic cross-sectional imaging modalities used for implant

Correspondence to: Mr Gainer Raúl Jasa. E-mail: Gainer@odon.edu.uy

The main funders of the study are the University of the Republic, Montevideo, Uruguay, and the Kyushu University, Fukuoka, Japan.
Received 2 August 2016; revised 12 December 2016; accepted 10 January 2017

planning,[4,10,11] and both have recently been replacing conventional panoramic radiographs.[1] CBCT requires a lower exposure dose than CT[12,13] and provides adequate image quality at a lower cost and with fewer artefacts than CT. CBCT has therefore become the ideal pre-operative assessment tool for dental implant surgery.[1,14]

The MC runs from the mandibular foramen to the mental foramen[15] and appears radiographically as a radiolucent zone lined by superior and inferior sclerotic borders.[16] However, the density and clarity of the MC borders vary among different people and even within the same individual, among parts on the same side.[3,16–18] One report found that MCs in the first molar region were not visible in 22.7% of cases using panoramic radiography and in 8.2% of cases using CBCT.[17] Oliviera-Santos et al[16] found that in the 47% of cases, identification of the MC was not readily feasible on a CBCT cross-sectional image. Conditions such as age and location exert a significant effect on the visibility of the MC, and better visibility of the MC is achieved in edentulous regions than in dentate regions.[18,19] These conditions could affect the visibility of the MC in panoramic radiography and CBCT images.

Exposure variables, such as tube current, tube voltage, size of the field of view (FOV) and full- or half-scan modes, can be altered with some CBCT scanners to improve image quality.[1,10,20] Higher tube currents decrease image noise, and higher tube voltages increase the mean energy of the X-ray beam. To a greater or lesser extent, both of these exposure parameters influence the patient dose and image quality by increasing or decreasing the amount and energy of photons. These effects on dose and image quality should be properly balanced, and the image quality should be analyzed using an objective method.[21] Image processing is routinely performed to extract important information that may not be seen by viewing only the axial image set. However, various parameters including slice or interval thickness are used in an almost completely arbitrary manner[22] without confirming whether it improves the diagnostic image quality.

Little is known about whether exposure and image-processing parameters influence the visibility of clear or unclear MCs in CBCT. The aim of this study was to investigate the influence of tube current, tube voltage and slice thickness on the visibility of MCs with different radiological appearances (clear and unclear MCs) in CBCT.

Methods and materials

Samples

The samples in this study comprised 12 dry human mandibles (24 half mandibles) with edentulous ridges posterior to the mental foramen, obtained from the Anatomy Museum of the School of Dentistry Department, University of the Republic, Uruguay. This research was approved by the Ethics Committee of the School of Dentistry, expedient number 091900-000071-11.

The samples were divided into 2 groups; 16 "clear" and 8 "unclear" based on the visibility of the MC walls in a previous CBCT study on the same samples (unpublished data). In that study, two observers examined the samples twice with an interval of 15 days, and the half mandibles were rotated on the horizontal axis in the sagittal plane, so that the MCs became horizontal in the sagittal view. The MC walls were then observed from mesial to distal in the cross-sectional view. At first, each observer noted whether the cortication of the MC was clearly visible, partially disrupted or completely disrupted, and then rated them as "clear", "partially clear" or "unclear", respectively. Finally, after consensus with a third specialist from the Department of Radiology, two groups of "clear" and "unclear" MCs were confirmed.

In the present study, the total length of the MC was divided into three sections of equal length on each half mandible by drawing four vertical lines with gutta-percha from the posterior margin of the mental foramen to the anterior margin of the mandibular foramen (Marks 1–4). For this research, we used the images at Mark 2 (first molar region) for observation, which is the most common site of insertion for endosseous implants.[2,3] Each half mandible was fixed within a container (18 cm in diameter and 7 cm in height) with the mandibular plane parallel to the floor, ensuring it was in an upright position (Figure 1). The containers were filled with water to simulate soft-tissue absorption and scatter radiation, and the height and width of the containers were larger than the FOV used.[23]

Image acquisition

Images of each half mandible were acquired using a CBCT system (CS 9300C Select; Carestream Health Inc., Marne-la-Vallée, France). At first, each half mandible was scanned with a wire inside the MC to identify the location of the MC. The exposure parameters were: FOV 10×5 cm (diameter $\times$ height); voxel size 0.18 mm; tube voltage 90 kV; tube current 4 mA; and exposure time 6.1 s. The wire was then removed without moving the sample, and the half mandibles were scanned using the same FOV and the same exposure time, but at varying tube voltages and currents. Scan parameters are summarized in Table 1. We performed analysis in two steps; Step 1 using almost equal exposure doses (90 kV/5 mA, 70 kV/10 mA and 60 kV/15 mA) to see the effect of tube voltages and that of slice thickness, and Step 2 using the same tube voltage (70 kV), but different currents (2 mA, 5 mA, 10 mA and 15 mA) to see the effects of tube currents. Thus, each half mandible was scanned 6 times, and a total of 144 scan conditions were obtained. Neither the sensor nor the mandibles was moved during scanning.

Sample image preparation for receiver-operating characteristic analysis

The images of each half mandible with wire were rotated on the horizontal axis, so that the MC became

Figure 1 A half mandible immersed in water and placed on the CBCT machine.

horizontal at Mark 2, and they were saved. These images were designated as the gold standard. The images of the same half mandibles without the wire were rotated using the same rotation angle. The data were then exported in digital imaging and communications in medicine format, with isotropic voxels of 0.18 mm and were imported for analysis with ImageJ software (National Institutes of Health, Bethesda, MD).

From axial slices of each scan, 100 slices (18 mm) of serial cross-sectional images were obtained at Mark 2. Subsequently, overlaid cross-sectional images with 5 different slice thicknesses were obtained using 1, 5, 11, 15 and 21 consecutive slices (Table 2), taking the mark as the centre. A region of interest of 8.1 × 8.1 mm was cropped on each overlaid cross-sectional image to prepare the images for observation. Referring to the gold standard images (mandible with wire), we cropped the images with and without the MC (Figure 2). In addition, the region of interest of the serial cross-sectional images of 100 slices with and without the MC was also cropped. Cropped images were randomly displayed on a personal computer in a quiet room with dim lighting. Overlaid and serial images were observed at different times by five oral and maxillofacial radiologists with experience in assessing images for the presence or absence of the MC. They were instructed to use a five-point scale, from "definitely not present" = 1 to "definitely present" = 5. Observations were performed twice at intervals of 2 weeks in the order set out below.

Step 1: Cropped images (720 overlaid and 144 serial images) of 3 combinations of exposure parameters were selected, which had almost equal exposure doses (90 kV/5 mA, 70 kV/10 mA and 60 kV/15 mA), using a calculated dose–area product for each combination. The dose–area product was obtained by X-ray dose emission information from the CS 9300 Family Safety, Regulatory and Technical Specifications (SM747) Ed04. These images were prepared to see the effect of tube voltages when comparing the overlaid images with the serial images, and to see the effect of the number of slices in the overlaid images.

Step 2: 4 sets of images (960 overlaid and 192 serial images) with the same tube voltage (70 kV), but different currents (2 mA, 5 mA, 10 mA and 15 mA) were examined to see the effects of tube current.

All variables were compared on clear and unclear MCs of all half mandibles.

Statistical analyses

Diagnostic accuracy was compared with the area under the curve (Az) of receiver-operating characteristic analysis, using ROCKIT v. 1.1B (Charles E Metz, University of Chicago, Chicago, IL). The significance of differences in the Az values among the different imaging protocols was analyzed by Tukey–Kramer test of all combinations of pairs in multiple comparisons and Mann–Whitney *U*-test for two samples using R Core Team (2015) [R: A language and environment for statistical computing (R Foundation for Statistical Computing, Vienna, Austria); available from: https://www.R-project.org/] with a significance level of 5%. Intra-observer agreement rates between the repeat observations were assessed with kappa values using three grades: 1 or 2, 3, and 4 or 5. Values <0.20 indicated poor agreement, 0.21–0.40 fair agreement, 0.41–0.60

Table 1 Scan parameters for CBCT

Scan parameter	*Variation*
Tube voltage (kV)	60, 70, 90
Tube current (mA)	2, 5, 10, 15
Scanning time (s)	6.1
FOV (diameter and height) (cm)	10 × 5
Voxel size (mm)	0.18

FOV, field of view.

Table 2 Slice thickness in millimetres (mm)

Number of slices	*Thickness (mm)*
1	0.18
5	0.90
11	1.98
15	2.70
21	3.78

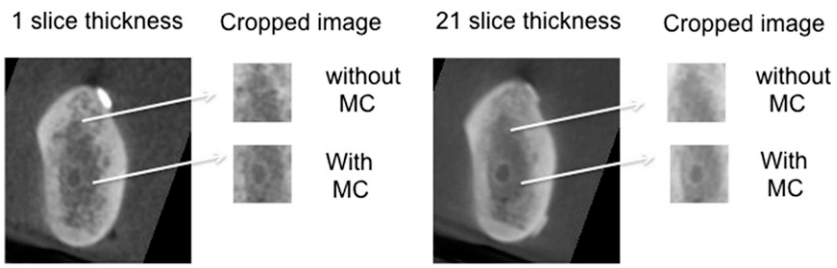

Figure 2 Examples of cropping of overlaid images (1 and 21 slice thicknesses). MC, mandibular canal.

moderate agreement, 0.61–0.80 good agreement and 0.81–1.00 excellent agreement.

Results

First, we confirmed whether the intraobserver agreement was sufficient or not. Using the same data sets as in Step 1 and Step 2, we calculated kappa values for this analysis. The average kappa value was 0.639, which showed that intraobserver agreement was good.

Figure 3 shows the Az values in the serial images (Figure 3a) and those in the overlaid images (Figure 3b) under similar doses. Az values in the serial images at 60 kV, 70 kV and 90 kV were 0.885, 0.935 and 0.938, respectively (Figure 3a), and those in the overlaid images were 0.791, 0.851 and 0.883, respectively (Figure 3b). Higher tube voltages led to higher Az values even under the same doses. There were significant differences between 60 kV and 90 kV ($p = 0.0330$) in the serial images (Figure 3a), and between 60 kV and 70 kV ($p = 0.0012$) and between 60 kV and 90 kV ($p < 0.0001$) in the overlaid images (Figure 3b).

We compared the Az values of clear and unclear MCs in the same images used above (Figure 4a; serial images, Figure 4b; overlaid images). The Az values of the clear and unclear MCs were 0.965 and 0.819, respectively, in the serial images (Figure 4a) and 0.872 and 0.787, respectively, in the overlaid images (Figure 4b). There were significant differences between the Az values in clear and unclear MCs ($p < 0.0001$) in both the serial and overlaid images.

Comparing the Az values for serial images and overlaid images in Figures 3 and 4, we observed that the diagnostic accuracy of the serial images was significantly higher than that of the overlaid images ($p < 0.0001$). A correlation was found between the serial and overlaid images of each half mandible (correlation coefficient of 0.69) (Figure 5).

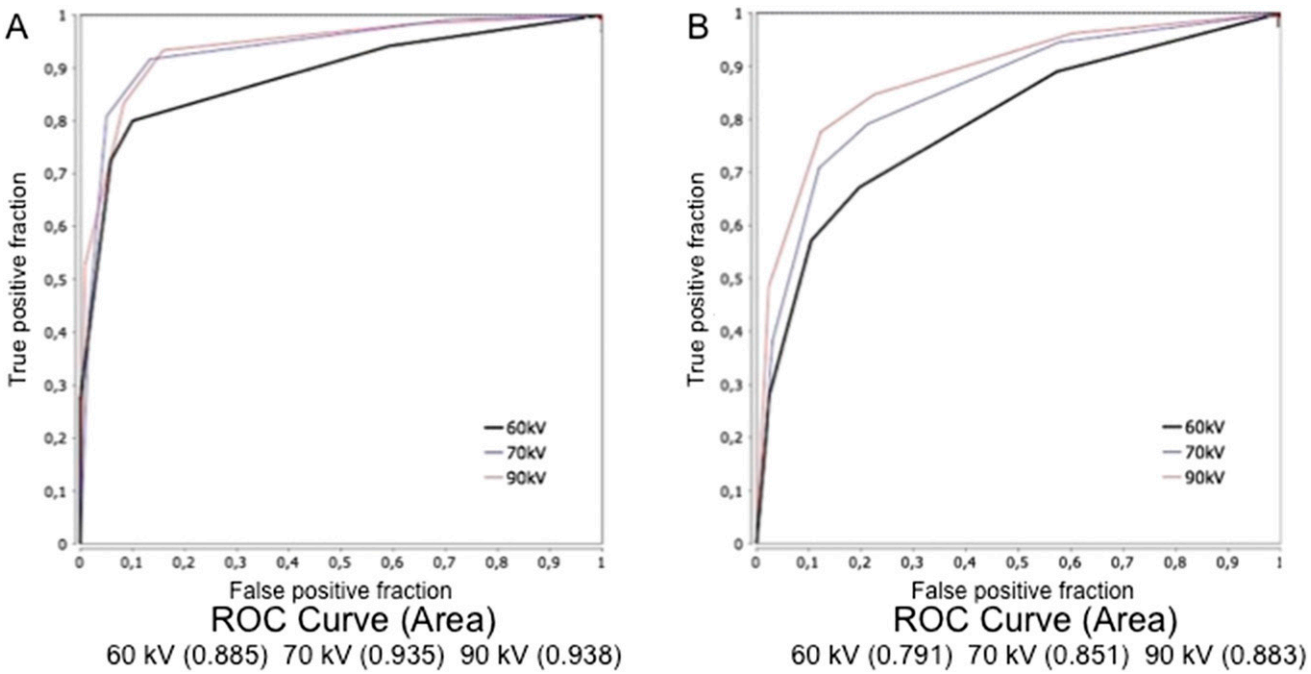

Figure 3 Receiver-operating characteristic (ROC) curves for different tube voltages (60, 70, 90 kV) under similar doses: (a) shows the area under the curve values of the observation in serial images, (b) shows those in overlaid images.

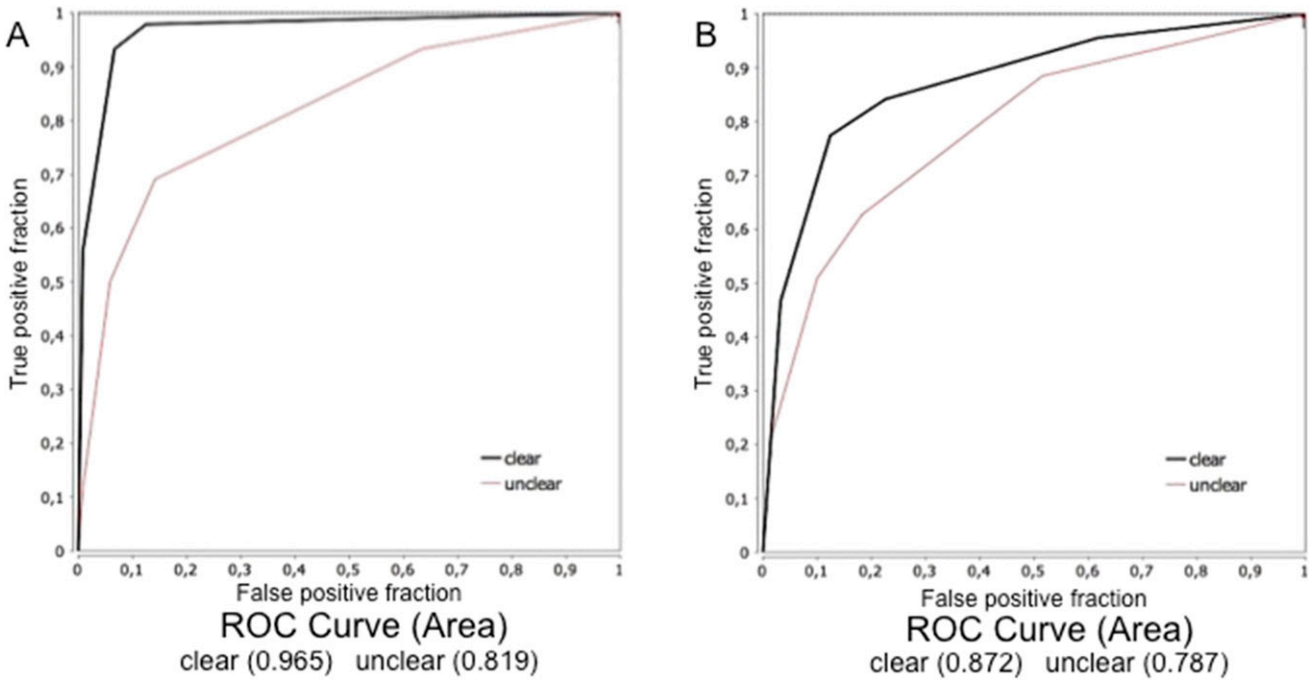

Figure 4 Receiver-operating characteristic (ROC) curves comparing the observation of clear mandibular canals (MCs) with that of unclear MCs under same doses: (a) shows the area under the curve values in serial images and (b) shows those in overlaid images.

Figure 6 shows the effect of the slice thickness of the overlaid images on the Az values. The Az values in the Step 1 images increased with thicker slices on clear (Figure 6a) and unclear MCs (Figure 6b), showing a significant difference between 1 and 21 slices in both ($p < 0.0001$). For clear MCs (Figure 6a), there were no significant differences among the three thickest slices ($p > 0.7517$). The Az values were 0.920 for the 11 slice thickness, 0.922 for the 15 slice thickness and 0.931 for the 21 slice thickness. For unclear MCs (Figure 6b), the Az values were lower than those for clear MCs and, in contrast to clear MCs, unclear MCs showed significant differences between thicker slices (11 and 15 slices, and 11 and 21 slices) ($p < 0.0423$).

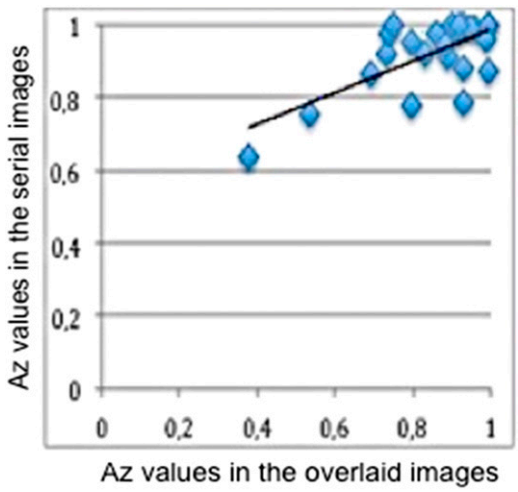

Figure 5 Correlation of area under the curve (Az) values between serial and overlaid images of each half mandible. Dots represent the Az values of receiver-operating characteristic analysis of each half mandible.

Figure 7 shows the influence of tube voltage on clear and unclear MCs in the serial images acquired under the same doses. The Az values with different tube voltages were similar on clear MCs: 0.947 at 60 kV, 0.982 at 70 kV and 0.976 at 90 kV (Figure 7a). There were no significant differences in the Az values among the three voltages ($p > 0.1200$), especially for high voltages between 70 kV and 90 kV ($p = 1.0000$). In contrast, the Az values of images of unclear MCs were low at 60 kV (0.759) compared with 70 kV (0.849) and 90 kV (0.857) (Figure 7b). However, there was no significant difference between the Az values of 60 kV and 90 kV ($p = 0.1000$).

We compared the Az values in the Step 2 images with different tube currents. The Az values increased when higher currents were used (Figure 8). Images with clear MCs (Figure 8a) recorded an Az value of 0.732 with a current of 2 mA, 0.943 with 5 mA, 0.985 with 10 mA and 0.989 with 15 mA. These values were much higher than those of images with unclear MCs (Figure 8b): 0.451 with a current of 2 mA, 0.731 with 5 mA, 0.866 with 10 mA and 0.897 with 15 mA. With high currents of 10 mA and 15 mA, there were no significant differences in Az values for either clear or unclear MCs ($p = 0.9340$, $p = 0.65594$); however, for clear MCs, the difference was smaller than that for unclear MCs. With lower currents of 5 mA and 10 mA, there was no significant difference in Az values ($p = 0.0730$) for clear MCs, while there was a significant difference ($p < 0.02876$) for unclear MCs. These differences can be seen in Figure 9.

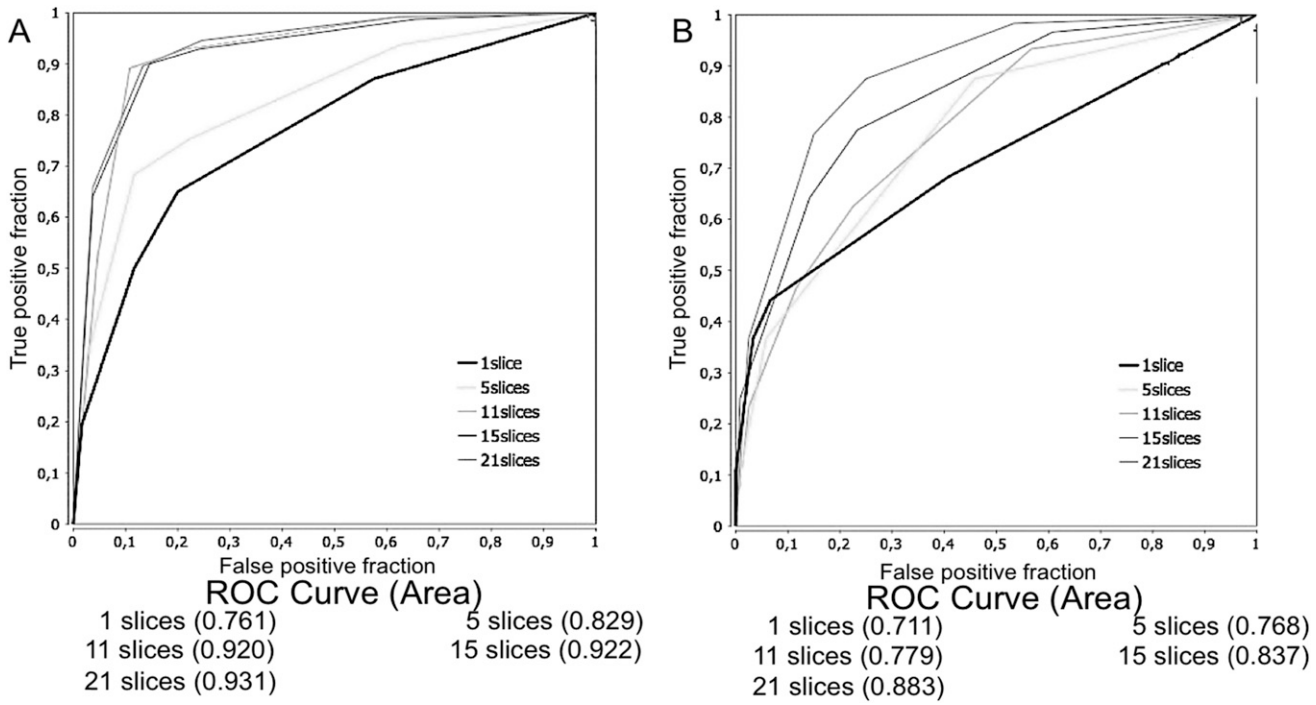

Figure 6 Receiver-operating characteristic (ROC) curves in overlaid images with different slice thicknesses (1, 5, 11, 15 and 21 slice thicknesses) under the same doses: (a) shows the area under the curve values for clear mandibular canals (MCs) and (b) shows those for unclear MCs.

Discussion

We evaluated the effects of exposure parameters and slice thickness on CBCT image quality for detecting MCs. It was verified that tube voltage, current and slice thickness affected the visibility of clear and unclear MCs in different ways. The first molar region (Mark 2) was selected in this study, because (1) implant surgery is often performed in this region,[2,4,24–26] (2) panoramic radiography and CBCT offer lower visibility in this

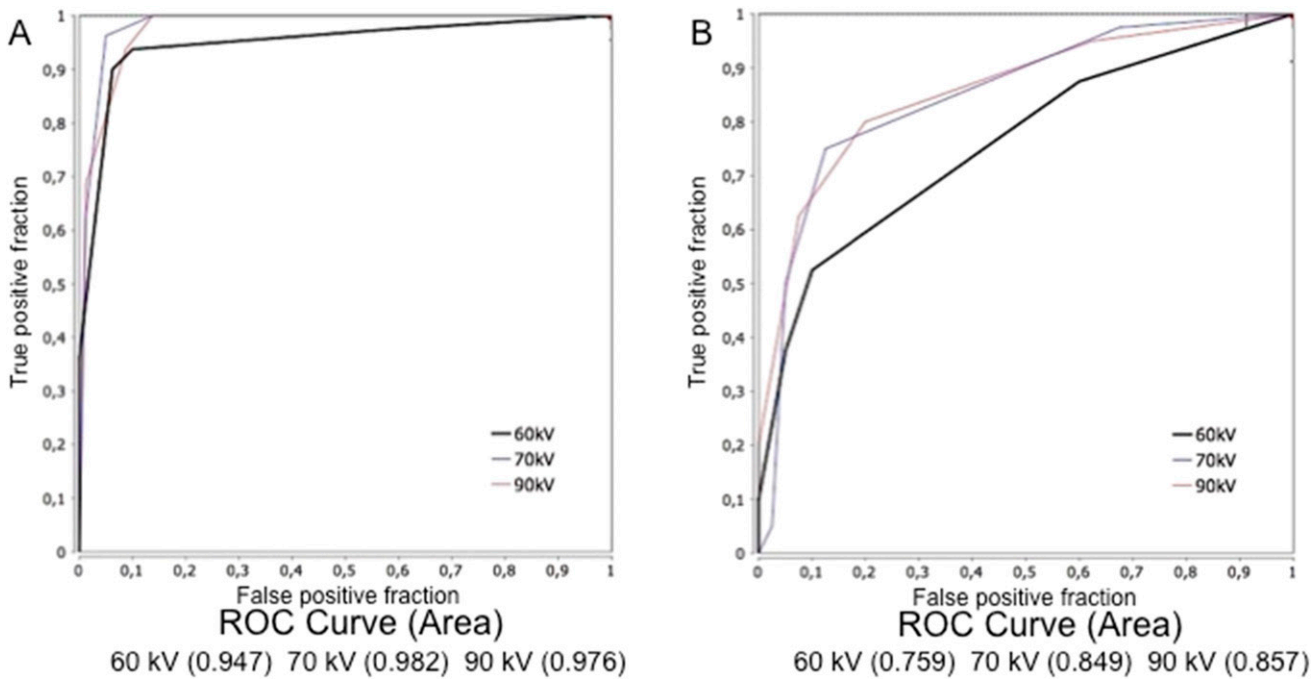

Figure 7 Receiver-operating characteristic (ROC) curves for different tube voltages (60 kV, 70 kV and 90 kV): (a) shows the area under the curve values for clear mandibular canals (MCs) and (b) shows those for unclear MCs.

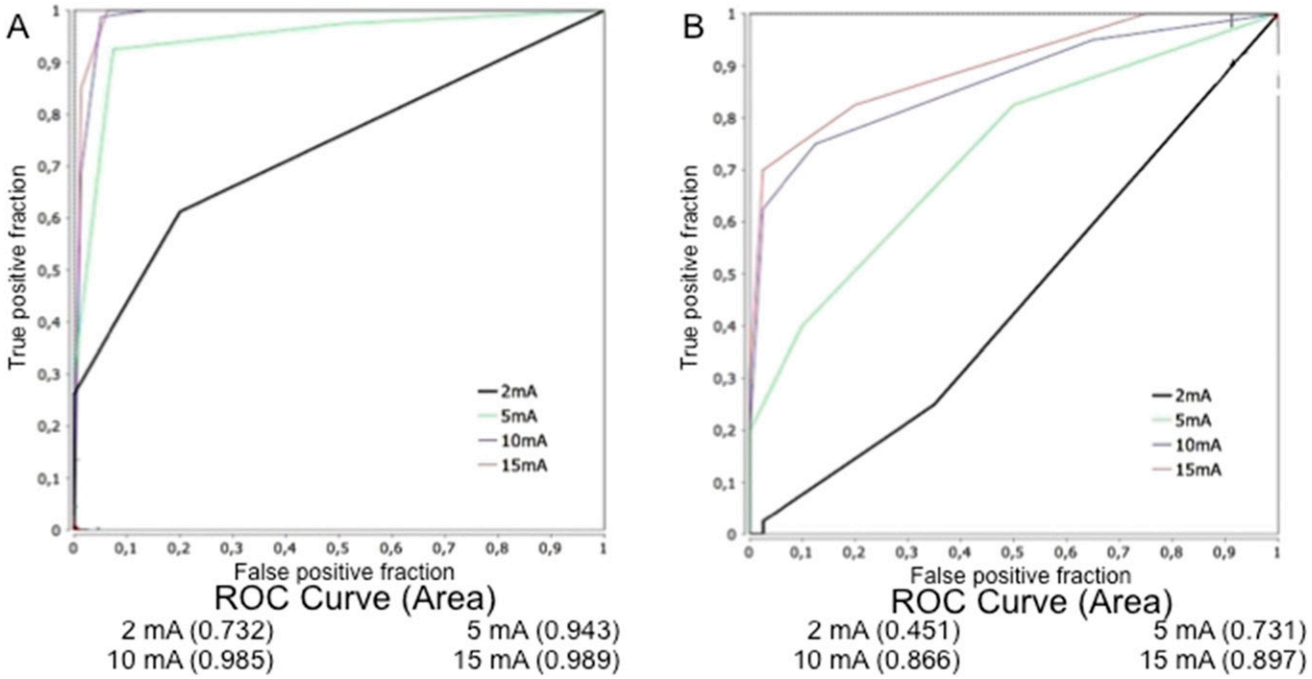

Figure 8 Receiver-operating characteristic (ROC) curves for different currents (2 mA, 5 mA, 10 mA and 15 mA) in serial images at 70 kV: (a) shows the area under the curve values for clear mandibular canals (MCs) and (b) shows those for unclear MCs.

region[3,17–19] and (3) this region was selected as the test region in another study[27] to evaluate different tomographic techniques.

When exposures with similar doses were used, serial images were better than overlaid images (Figures 3 and 4). There was a correlation between serial and overlaid images (Figure 5); therefore, when serial images cannot be obtained, we suggest using overlaid images with thicker slices (Figure 6).

Our study showed that slice thicknesses affected the visibility of MCs in the reconstructed images. Az values increased significantly with slice thicknesses from 0.18 mm (1 slice) to 3.78 mm (21 slices) ($p < 0.0001$), especially in unclear MCs (Figure 6). Chadwick and

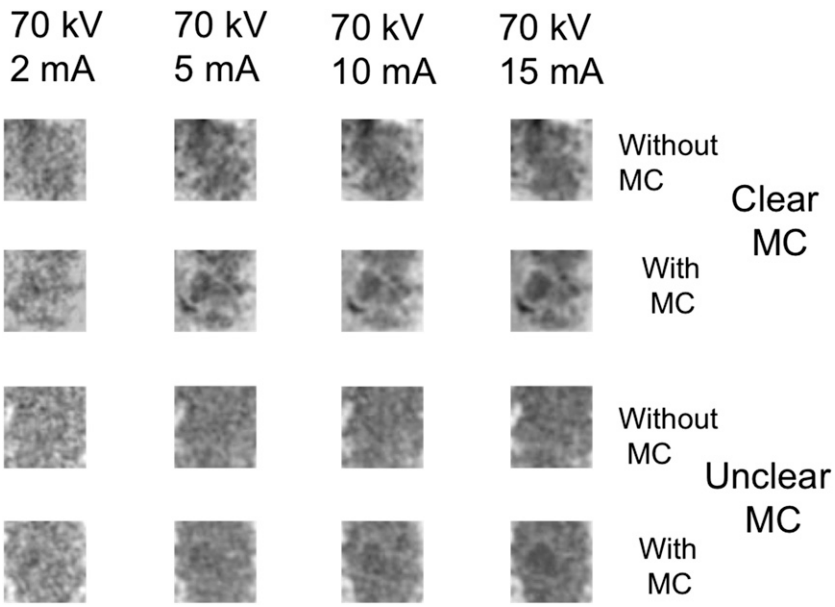

Figure 9 Cropped images with and without mandibular canals (MCs) at various tube currents in combination with 70 kV with clear (top) and unclear (bottom) MCs.

Lam's[22] work suggested that when overlaid images are used for diagnosis, relatively thicker slices should be used. Ekestubbe et al[28] noted that conventional spiral tomography simplifies the identification of structures with thin borders such as the MC, because they produce images with 4.00-mm slice thickness and the scanning plane is perpendicular to the MCs. Lofthag-Hansen et al[27] proposed the hypothesis that if 2-mm-thick slices are used, the clarity of the MCs would be greater than that for 1-mm-thick slices. These reports are consistent with our results. Pauwels et al[29] stated that image noise can be reduced by averaging multiple consecutive slices. Our results also showed that with thicker slices, the image noise was reduced (Figure 2). Thus, to see MCs, it is better to use thicker slices, especially for unclear MCs.

Svenson et al[30] concluded that the variation in diagnostic accuracy depends on exposure dose, whereas the effect of tube voltage is practically negligible. In contrast, Pauwels et al[21] used a combination of tube currents (1–8 mA) and tube voltages (60 kV, 70 kV, 80 kV and 90 kV) and found an increase in the contrast-to-noise ratio at the highest tube voltage (90 kV) when the radiation dose was fixed. Another study by Pauwels et al,[31] in which bone structure was analyzed and the same exposure dose was used, showed that the contrast-to-noise ratio with the highest tube voltage protocol (90 kV) was significantly different from that with lower tube voltage settings (63 kV and 74 kV). Our study showed that the visibility of MCs was strongly affected by tube voltage and tube current, especially for unclear MCs, for which the highest tube voltage (90 kV) produced the largest Az value of 0.857 (Figure 7b). These results support the findings of Pauwels et al.[31]

High tube currents were needed to achieve better image quality for detecting MCs (Figure 8). Panmekiate et al[10] acquired 160 CBCT data sets with 8 different combinations of 4 kinds of tube voltages (60 kV, 80 kV, 100 kV and 120 kV), 2 kinds of tube currents (10 mA and 15 mA) and a scan time of 14 s. They took linear measurements between the inner surfaces of the MC walls and the mandibular points and found no significant differences among all the images. In consideration of the dose reduction, they suggested that 10 mA and 60 kV should be used. In the present study, our results were similar to those of Panmekiate et al[10] for clear MCs, but relatively higher voltages and currents were needed to see unclear MCs. Neves et al[32] acquired images with a scan time of 10.8 s at 60 kV, with seven different combinations of tube currents (2 mA, 4 mA, 6.3 mA, 8 mA, 10 mA, 12 mA and 15 mA). As in our study, they found that the image quality increased concomitantly with the tube current. However, they concluded that the best low-dose protocol with good image quality was obtained with the 10 mA setting. From the results of Figures 7 and 8, we suggest using 5 mA and 70 kV for clear MCs, and 10 mA and 70 kV for unclear MCs, since there was no significant difference between 5 mA and 10 mA for clear MCs ($p = 0.0730$) and between 10 mA and 15 mA for unclear MCs ($p = 0.6560$) to keep the dose as low as reasonably achievable (the so-called ALARA principle), based on Neves et al's study.[32]

In the present study, we recognized that when previous panoramic radiographs of the patients were available, it was important to know whether MCs in them are clear or unclear before taking and processing CBCT images, because the most suitable dose and image-processing method depend on this information. Even in edentulous regions, which are reported to have better visibility of MCs,[19] we should increase the exposure parameters in cases in which the MC is unclear. Some studies[16,17] suggest that if the MC is not well visualized in one technically satisfactory examination, it would be difficult to identify the MC using other imaging modalities. Based on our results, we suggest that the use of a higher tube current, higher tube voltage and thicker slices will improve the visibility of the MC, when it has been poorly depicted in previous examinations.

Conclusions

Serial images are better than overlaid images for detecting MCs, and slices thicker than 1 mm should be used for image processing when overlaid images are used. When patients have clear MCs in previous panoramic radiographs, lower exposure parameters can be used to reduce the radiation dose. In contrast, for unclear MCs, higher voltages and currents are required.

References

1. Rustemeyer P, Streubuhr U, Suttmoeller J. Low-dose dental computed tomography: significant dose reduction without loss of image quality. *Acta Radiol* 2004; **45**: 847–53. doi: https://doi.org/10.1080/02841850410001402
2. Takahashi A, Watanabe H, Kamiyama Y, Honda E, Sumi Y, Kurabayashi T. Localizing the mandibular canal on dental CT reformatted images: usefulness of panoramic views. *Surg Radiol Anat* 2013; **35**: 803–9. doi: https://doi.org/10.1007/s00276-013-1120-6
3. Angelopoulos C, Thomas SL, Hechler S, Parissis N, Hlavacek M. Comparison between digital panoramic radiography and cone-beam computed tomography for the identification of the mandibular canal as part of presurgical dental implant assessment. *J Oral Maxillofac Surg* 2008; **66**: 2130–5. doi: https://doi.org/10.1016/j.joms.2008.06.021
4. Hsu JT, Huang HL, Fuh LJ, Li RW, Wu J, Tsai MT, et al. Location of the mandibular canal and thickness of the occlusal cortical bone at dental implant sites in the lower second premolar and first molar. *Comput Math Methods Med* 2013; **2013**: 608570. doi: https://doi.org/10.1155/2013/608570
5. de Oliveira Júnior MR, Saud AL, Fonseca DR, De-Ary-Pires B, Pires-Neto MA, de Ary-Pires R. Morphometrical analysis of the human mandibular canal: a CT investigation. *Surg Radiol Anat* 2011; **33**: 345–52. doi: https://doi.org/10.1007/s00276-010-0708-3

6. Noujeim M, Prihoda T, Langlais R, Nummikoski P. Evaluation of high-resolution cone beam computed tomography in the detection of simulated interradicular bone lesions. *Dentomaxillofac Radiol* 2009; **38**: 156–62. doi: https://doi.org/10.1259/dmfr/61676894
7. Jasa GR, Vizzotto MB, da Silveira PF, da Silveira HD, da Silveira HD, Ruhland LR, et al. Buccal-lingual localization of the mandibular canal in relationship with the third molar using the lateral oblique technique. *J Oral Maxillofac Radiol* 2014; **2**: 15–20.
8. Delamare EL, Liedke GS, Vizzotto MB, da Silveira HD, de Azambuja TW, da Silveira HD. Topographic relationship of impacted third molars and mandibular canal: correlation of panoramic radiograph signs and CBCT images. *Braz J Oral Sci* 2012; **11**: 411–15.
9. Benediktsdottir IS, Hintze H, Petersen JK, Wenzel A. Accuracy of digital and film panoramic radiographs for assessment of position and morphology of mandibular third molars and prevalence of dental anomalies and pathologies. *Dentomaxillofac Radiol* 2003; **32**: 109–15. doi: https://doi.org/10.1259/dmfr/15999089
10. Panmekiate S, Apinhasmit W, Peterson A. Effect of electric potential and current on mandibular linear measurements in cone beam CT. *Dentomaxillofac Radiol* 2012; **41**: 578–82. doi: https://doi.org/10.1259/dmfr/51664704
11. Naitoh M, Nakahara K, Suenaga Y, Gotoh K, Kondo S, Ariji E. Comparison between cone-beam and multislice computed tomography depicting mandibular neurovascular canal structures. *Oral Surg Oral Med Oral Pathol Oral Radiol Endod* 2010; **109**: 25–31. doi: https://doi.org/10.1016/j.tripleo.2009.08.027
12. Tyndall DA, Brooks SL. Selection criteria for dental implant site imaging: a position paper of the American Academy of Oral and Maxillofacial Radiology. *Oral Surg Oral Med Oral Pathol Oral Radiol Endod* 2000; **89**: 630–7.
13. Loubele M, Bogaerts R, van Dijck E, Pauwels R, Vanheusden S, Suetens P, et al. Comparison between effective radiation dose of CBCT and MSCT scanners for dentomaxillofacial applications. *Eur J Radiol* 2009; **71**: 461–8. doi: https://doi.org/10.1016/j.ejrad.2008.06.002
14. Leite GM, Lana JP, de Carvalho Machado V, Manzi FR, Souza PE, Horta MC. Anatomic variations and lesions of the mandibular canal detected by cone beam computed tomography. *Surg Radiol Anat* 2014; **36**: 795–804. doi: https://doi.org/10.1007/s00276-013-1247-5
15. Hass LF, Dutra K, Porporatti AL, Mezzomo LA, De Luca Canto G, Flores-Mir C, et al. Anatomical variations of mandibular canal detected by panoramic radiography and CT: a systematic review and meta-analysis. *Dentomaxillofac Radiol* 2016; **45**: 20150310.
16. Oliveira-Santos C, Capelozza AL, Dezzoti MS, Fischer CM, Poleti ML, Rubira-Bullen IR. Visibility of the mandibular canal on CBCT cross-sectional images. *J Appl Oral Sci* 2011; **19**: 240–3.
17. Jung YH, Cho BH. Radiographic evaluation of the course and visibility of the mandibular canal. *Imaging Sci Dent* 2014; **44**: 273–8. doi: https://doi.org/10.5624/isd.2014.44.4.273
18. Kamrun N, Tetsumura A, Nomura Y, Yamaguchi S, Baba O, Nakamura S, et al. Visualization of the superior and inferior borders of the mandibular canal: a comparative study using digital panoramic radiographs and cross-sectional computed tomography images. *Oral Surg Oral Med Oral Pathol Oral Radiol* 2013; **115**: 550–7. doi: https://doi.org/10.1016/j.oooo.2013.01.001
19. Miles MS, Parks ET, Eckert GJ, Blanchard SB. Comparative evaluation of mandibular canal visibility on cross-sectional cone-beam CT images: a retrospective study. *Dentomaxillofac Radiol* 2016; **45**: 20150296. doi: https://doi.org/10.1259/dmfr.20150296
20. Sur J, Seki K, Koizumi H, Nakajima K, Okano T. Effects of tube current on cone-beam computerized tomography image quality for presurgical implant planning *in vitro*. *Oral Surg Oral Med Oral Pathol Oral Radiol Endod* 2010; **110**: 29–33. doi: https://doi.org/10.1016/j.tripleo.2010.03.041
21. Pauwels R, Silkosessak O, Jacobs R, Bogaerts R, Bosmans H, Panmekiate S. A pragmatic approach to determine the optimal kVp in cone beam CT: balancing contrast-to-noise ratio and radiation dose. *Dentomaxillofac Radiol* 2014; **43**: 20140059. doi: https://doi.org/10.1259/dmfr.20140059
22. Chadwick JW, Lam EW. The effects of slice thickness and interslice interval on reconstructed cone beam computed tomographic images. *Oral Surg Oral Med Oral Pathol Oral Radiol Endod* 2010; **110**: 37–42. doi: https://doi.org/10.1016/j.tripleo.2010.05.008
23. Oliveira ML, Freitas DQ, Ambrosano GM, Haiter-Neto F. Influence of exposure factors on the variability of CBCT voxel values: a phantom study. *Dentomaxillofac Radiol* 2014; **43**: 20140128. doi: https://doi.org/10.1259/dmfr.20140128
24. Kinoshita H, Nakahara K, Matsunaga S, Usami A, Yoshinari M, Takano N, et al. Association between the peri-implant bone structure and stress distribution around the mandibular canal: a three-dimensional finite element analysis. *Dent Mater J* 2013; **32**: 637–42. doi: https://doi.org/10.4012/dmj.2012-175
25. Misch CM. Use of the mandibular ramus as a donor site for onlay bone grafting. *J Oral Implantol* 2000; **26**: 42–9. doi: https://doi.org/10.1563/1548-1336(2000)026<0042:UOTMRA>2.3.CO;2
26. Kamburoglu K, Murat S, Kiliç C, Yuksel S, Avsever H, Farman A, et al. Accuracy of CBCT images in the assessment of buccal marginal alveolar peri-implant defects: effect of field of view. *Dentomaxillofac Radiol* 2014; **43**: 20130332.
27. Lofthag-Hansen S, Gröndahl K, Ekestubbe A. Cone-beam CT for preoperative implant planning in the posterior mandible: visibility of anatomic landmarks. *Clin Implant Dent Relat Res* 2009; **11**: 246–55. doi: https://doi.org/10.1111/j.1708-8208.2008.00114.x
28. Ekestubbe A, Grondahl K, Ekholm S, Johansson PE, Grondahl HG. Low-dose tomographic techniques for dental implant planning. *Int J Oral Maxillofac Implants* 1996; **11**: 650–9.
29. Pauwels R, Araki K, Siewerdsen JH, Thongvigitmanee SS. Technical aspects of dental CBCT: state of the art. *Dentomaxillofac Radiol* 2015; **44**: 20140224. doi: https://doi.org/10.1259/dmfr.20140224
30. Svenson B, Welander U, Anneroth G, Soderfeldt B. Exposure parameters and their effects on diagnostic accuracy. *Oral Surg Oral Med Oral Pathol* 1994; **78**: 544–50. doi: https://doi.org/10.1016/0030-4220(94)90050-7
31. Pauwels R, Faruangsaeng T, Charoenkarn T, Ngonphloy N, Panmekiate S. Effect of exposure parameters and voxel size on bone structure analysis in CBCT. *Dentomaxillofac Radiol* 2015; **44**: 20150078. doi: https://doi.org/10.1259/dmfr.20150078
32. Neves FS, de Camargo T, de Azevedo Vaz SL, Campos PS, Bóscolo FN. Influence of cone-beam computed tomography milliamperage settings on image quality of the mandibular third molar region. *Oral Radiol* 2014; **30**: 27–31. doi: https://doi.org/10.1007/s11282-013-0132-6